Mobile On Demand COVID-19 Vaccine Production Units for Developing Countries - Supplementary Information

Steffen Fahr[ag], Samantha Ayde Peña-Benavides[bd], Lukas Thiel[a], Carl Sengoba[a], Kaan Karacasulu[a], Nina Ihling[c], Juan Eduardo Sosa-Hernández[d], Gary Gilleskie[f], John M. Woodley[b], Roberto Parra-Saldivar[d]*, Seyed Soheil Mansouri[b]*, Kosan Roh[ae1]

[a] Process Systems Engineering (AVT.SVT), RWTH Aachen University, 52074 Aachen, Germany

[b] Department of Chemical and Biochemical Engineering, Technical University of Denmark, DK-2800 Kongens Lyngby, Denmark

[c] Biochemical Engineering (AVT.BioVT), RWTH Aachen University, 52074 Aachen, Germany

[d] Tecnologico de Monterrey, School of Engineering and Sciences, Monterrey, 64849, Mexico

[e] Department of Chemical Engineering and Applied Chemistry, Chungnam National University, 34141 Daejeon, Republic of Korea

[f] Golden LEAF Biomanufacturing Training and Education Center (BTEC), NC State University, 27606 Raleigh, NC, USA

[g] Institute of Plant and Process Technology, Technical University of Munich, 85748 Garching, Germany

1 Process Descriptions

This section covers descriptions of the mRNA and yeast process including process flow diagrams and a discussion of their implementation at MOD scale.

1.1 MOD mRNA vaccine Production

An mRNA production process was developed based on the literature and adapted for MOD manufacture. A schematic representation of the process is given in Fig. 1. Similar production processes to the one developed herein can be found in previous scientific and patent literature [2, 30, 45]. The process suggested in this work is scaled to produce up to 1 g pure mRNA per batch, which is equivalent to 10,000 doses (100 μg per dose) of the Moderna vaccine or 33,333 doses (30 μg per dose) of the BioNTech/Pfizer vaccine. The production of one batch is completed within two 8-hour shifts.

[1]Corresponding authors: R. Parra-Saldivar, E-mail: r.parra@tec.mx; S. S. Mansouri, E-mail: seso@kt.dtu.dk; K. Roh, E-mail: ksroh@cnu.ac.kr

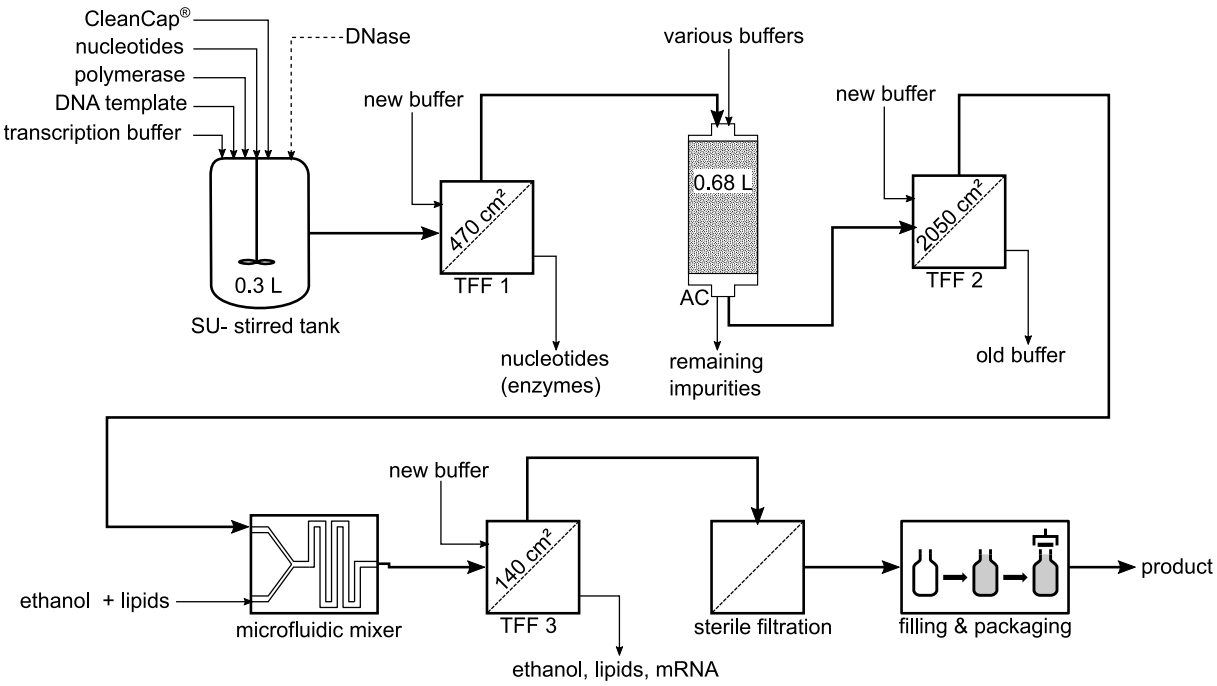

Fig. 1: Schematic representation of the mRNA Process. Abbreviations: single-use (SU), tangential flow filtration (TFF), affinity chromatography (AC).

The starting point of the process is assumed to be a linearised DNA template containing the desired genetic information, that is, in the case of COVID-19, a promoter and an untranslated region followed by the spike protein gene, another untranslated region, a Poly-A tail and a terminator [23]. The DNA is transcribed by the addition of a polymerase and nucleotides and suitable buffer in a disposable stirred tank of 0.3 L working volume (top left in Fig. 1). Among the nucleotides, modified uridine triphosphate (UTP) may be used as opposed to wild-strain UTP, as it reduces the innate immune response of cells and helps to control immune-activity of the therapeutic mRNA [37, 55]. Furthermore, a capping agent, such as the commercially available agent CleanCap®, is added for co-transcriptional capping. Capping increases translational efficiency and stability of the mRNA inside the target cell and thereby leads to a higher protein yield *in vivo* [42, 43, 49]. The reaction takes place in batch mode at 37 °C and is terminated after three hours by the addition of DNase I. After the reaction has finished, the mixture contains the desired mRNA, residual nucleotides, DNA fragments, enzymes, and side products. The main side products are abortive transcripts [12, 56] and double stranded (ds) RNA. dsRNA induces an innate immune response and thereby severely compromises the vaccine's efficacy [27].

In the small-scale process, the reactor effluent is manually transferred to the first unit of the downstream

process. All containers, cartridges, columns and tubing used in downstream processing are manufactured from single use materials. The first downstream operation, a transmembrane flow filtration (TFF), aims at concentrating the product, removing small impurities, such as nucleotides and abortive transcripts, and changing the buffer to one that is suitable for the next purification step. The molecular weight cutoff is chosen at around 2/3 of the molecular weight of the product [3]. Accordingly, a part of the enzymes in the mixture may be removed as well. The core of the downstream process is a pre-filled affinity chromatography (AC) column, which selectively separates the product from the remaining impurities. Oligo-dT affinity resin is commercially available and well-suited to separate the target mRNA from the rest of the mixture based on its Poly-A tail binding to immobilised Oligo-dT groups. A product yield of 92 % is assumed according to [25]. Further, the specific binding capacity is assumed to be 2 mg mRNA $mL^{-}1$ resin, based on the specification given by the manufacturer of the POROS™ Oligo-dT resin [47]. Following the affinity chromatography, the product stream is free of the aforementioned impurities and undergoes a buffer change in a second TFF unit before being transferred to the formulation unit.

As the mRNA itself is easily degraded by RNAse, mRNA vaccines rely on a vehicle, such as LNP, to protect the mRNA until it has reached the target cell. The encapsulation in LNP leads to better thermostability, reduced degradation in the human body, and enhanced uptake by the human cell [13, 21, 29, 51]. LNP can be formed through microfluidic mixing of different functional lipids soluted in ethanol with the aqueous mRNA-containing solution. Devices to carry out the mixing are commercially available, e.g., from Precision Nanosystems [40, 44] and Dolomite Microfluidics [4, 19]. The lipid composition used in this work is adapted from the one used in the Moderna COVID-19 vaccine [14, 22]. The product of the mixing step is transferred to the third TFF, where the LNP are retained while ethanol, unincorporated lipids, and mRNA permeate through the membrane. For regulatory reasons, the product is subject to a final sterile filtration through a 0.2 μm sterile filter, which retains potential remaining impurities, while the LNPs pass through it [2]. The final product is filled into vials (10 doses per vial). Filling and packaging can take place in a commercially available unit, such as the one offered by Watson Marlow [52].

Alternative downstream sequences have been developed for the purification of mRNA and usually rely on two to three different separation mechanisms, such as ionic interaction [3, 30], size exclusion [2, 3, 30], hydrophobic interaction [3, 45, 53] and affinity interaction [2].

Peripheral tasks, such as utility delivery, maintaining a cleanroom environment, and quality control, take place in the two containers. One important peripheral task is the provision of RNase-free water. Buffers

are mixed onsite with RNase-free water produced onsite to save storage capacity. Drinking water is required as a raw material and is treated by reverse osmosis and a subsequent ultrafiltration through a 5,000 Da membrane following [46]. Finally, room and equipment for cold storage of raw materials and product as well as ambient storage of SUE is included in the space and economic considerations. The available storage space enables to produce up to 100 full-sized batches (e.g., 1 Mio doses of 100 μg mRNA) without resupply, except for water and electricity.

Providing a comprehensive guideline on quality control is outside the scope of this work. However, an exemplary quality control strategy for the mRNA is developed to estimate its costs and its space requirements. mRNA quality control may include using DNA fluorescent dye and UV absorbance for verifying the absence of DNA and enzymes and quantifying the concentration of the mRNA [39]. The absence of dsRNA can exemplarily be proven by using dot blot [27]. Dynamic light scattering can be employed to monitor the size of LNP in the final product [16].

1.2 MOD Yeast-based Vaccine Production

The yeast-based process begins with the inoculum preparation. A cryovial containing yeast is thawed for 4 hours and inoculated in a shaking flask containing 250 mL of media, at 30 °C for 24 hours. The starter culture is then scaled-up, from 2 L to 10 L, corresponding to the working volume of the fermentation, as seen in Figure 2.

The fermentation process of the yeast *K. phaffii* to produce recombinant proteins usually consists of three phases. First, a glycerol (carbon source) batch phase for biomass growth, followed by a fed-batch glycerol phase to increase cell density, and finally a fed-batch methanol induction phase to produce the protein of interest [24, 48]. However, some studies suggest a two-phase process or a diauxic fermentation: a glycerol phase and an induction phase, avoiding the intermediate glycerol fed-batch phase. This modification is convenient as it simplifies the upstream process without compromising the product yield [28, 32]. Therefore, a two-phase fermentation process was implemented. The batch stage produces a high concentration of biomass [5]. Protocols recommend having 38 - 113 g L^{-1} cell dry weight (CDW) or its equivalent, 150 - 450 g L^{-1} wet cell weight (WCW) at the end of this stage, as it is a relevant factor for protein production [24, 48]. The final WCW in the process of RBD219-N1 was around 400 g L^{-1}. [7, 32]. Afterwards, methanol is fed during the induction phase for 70 hours and the cells secrete the protein of interest into the liquid media, which facilitates the following downstream steps because cell lysis is not

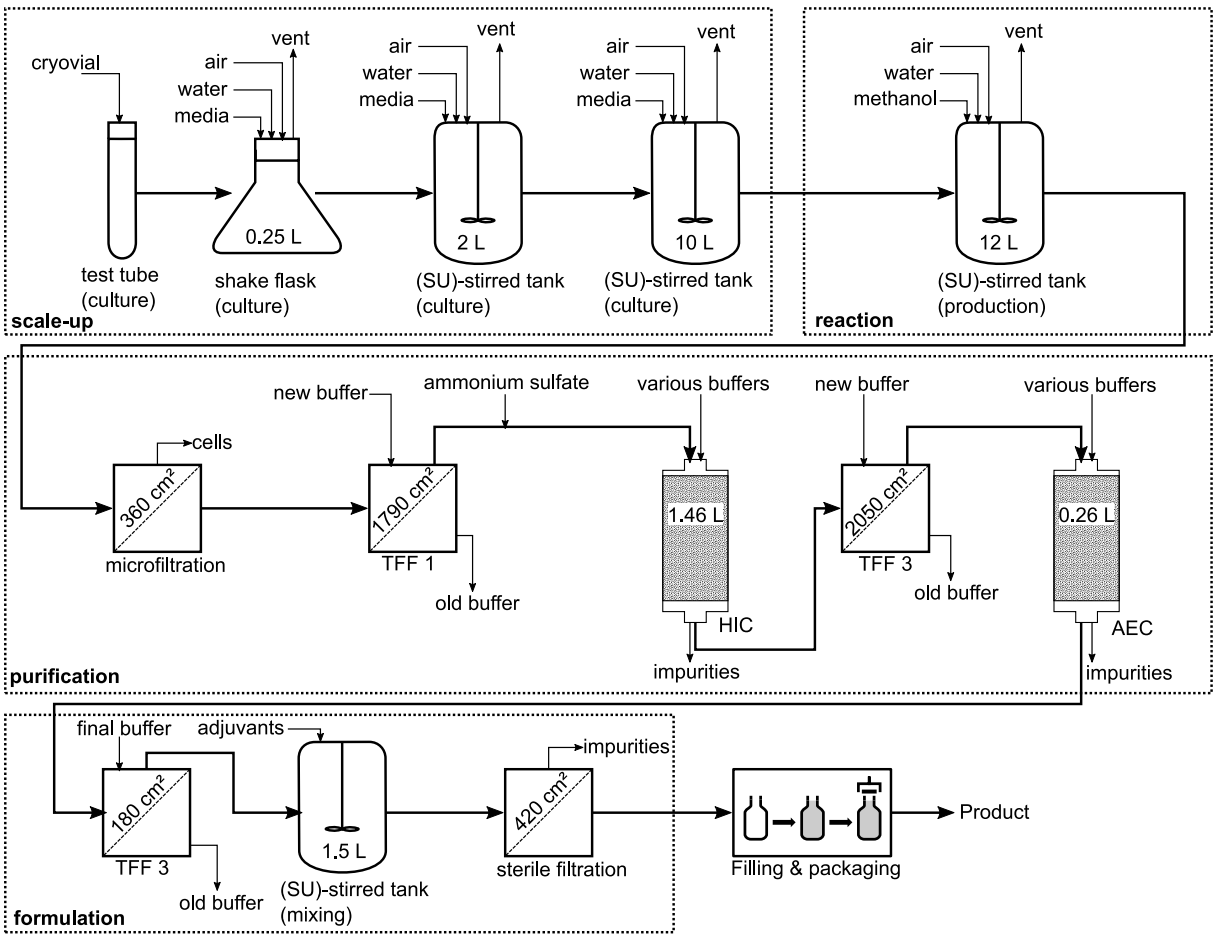

Fig. 2: Schematic representation of the yeast process.

required [41, 50]. The expected protein concentration is around 135 mg L^{-1} [7, 32].

The antigen purification starts with a filtration step to separate the liquid containing the protein from the solid biomass. This can be done by depth filtration in tandem or tangential flow microfiltration. TFF microfiltration was chosen because it efficiently removes yeast cells and occupies less space. The calculated area for this filter by SuperPro Designer was 360 cm^2. The remaining biomass in the feed is removed with a 0.45 μm filter (area of 0.179 m^2, according to SuperPro) as yeast cells have a size between 7 and 10 μm [34], achieving a recovery of 95 % [26]. Fine yeast particles of 0.5 - 1 μm might be in the filtrate, but the subsequent purification steps retain these impurities [34]. Afterwards, the protein (MW around 30 KDa) is concentrated using a 5 kDa membrane, achieving a recovery of 98 % as shown in [7]. Then, ammonium sulfate is added to the filtration retentate. This step is used to concentrate, clean-up, and stabilise the protein without denaturation. Conveniently, the concentrated retentate can be applied directly to the

next unit operation, hydrophobic interaction chromatography (HIC), because of its high salt level [9]. In HIC, the protein is captured using a butyl sepharose resin [32]. The binding capacity of the protein is 4.5 mg RBD $mL^{-}1$ resin [7], which results in a column volume of 1.46 L. The protein is eluted with 0.4 M ammonium sulfate in 30 mM Tris-HCl and the recovery in this unit was assumed to be 67 % according to [32]. Since the HIC elution pool has a high salt concentration, ultrafiltration-diafiltration (UF-DF) is employed to exchange the elution buffer with the formulation buffer, which corresponds to 20 mM Tris-HCl and 100 mM NaCl. This unit also concentrates the protein present in the eluate by using a 5 kDa MWCO membrane. The membrane area calculated by SuperPro is 0.205 m^2, which is in the range found in the studies done by Baylor College of Medicine [7, 32]. The retentate from the previous unit is polished by using anion-exchange chromatography (AEC), which is operated as negative capture. The equipment is pre-equilibrated with the same formulation buffer (pH 7.5) as before. The contaminants are bound to a Q Sepharose resin and the flow-through contains the protein of interest. The volume calculated by SuperPro for this column was 0.26 L and the recovery of this step is 78 % [32]. Lastly, the formulated bulk is sterile-filtered using a 0.22 μm disposable membrane filter, its area correspond to 176 cm^2. A recovery of 98 % was assumed for this step [17]. Protein subunit vaccines are formulated with adjuvants to elicit a stronger immune response. Alum is the most commonly used adjuvant in vaccines globally, and it is inexpensive [38]. Nevertheless, most COVID-19 protein-based vaccines contain a second adjuvant, namely CpG 1018, to balance the immune response [38]. After the bulk antigen is sterile filtered, it is adjuvanted with Alhydrogel 2 (aluminum hydroxide gel, also known as alum) and CpG 1018 in a mixer. Chen *et al.* [8] showed that 100 % of the antigen binds to alum. Moreover, CpG 1018 also binds easily to aluminum hydroxide, making it adequate for co-formulation with protein subunit vaccines [38]. Hence this step was assumed to have a yield of a 100 % (no protein loss). After the formulation step, the solution is sterile-filtered again with a 0.22 μm disposable filter. The area was calculated to be 420 cm^2. The biopharmaceutical can now be stored at 2-8 °C. The adjuvant CpG 1018 may be proprietary substance and it contributes significantly to the final cost per dose. Its cost contribution was approximated by the cost of "Fill/finish" per dose published by [11]. We used the higher-end estimation (1.5 USD or 1.33 €) per dose, which means that 500 μm of CpG 1018 account for 1.33 euros, making this adjuvant the most expensive raw material (95.46 % of the material costs). Other protein subunit vaccines produced in yeast against COVID-19 are adjuvanted with only alum, as it is the case of the Abdala vaccine developed by the Center for Genetic Engineering and Biotechnology (CIGB) in Cuba [33].

Quality control is highly relevant for vaccine production. According to the good manufacturing practices for biological products by the WHO [1], the manufacture process of biological products should follow the requirements of a pharmaceutical quality system (PQS). In particular, it is relevant to use analytical techniques that identify different physicochemical properties of the recombinant protein, such as size, amino acid sequence and hydrophobicity. Moreover, posttranslational modifications have to be identified and characterised, especially in yeast-based platforms, as the glycosylation profile is not necessarily the same as that of mammalian or human cell lines. Purity should be evaluated as shown by [32] and [8]. Aggregates, including dimers and other multiples of the desired product should be investigated. Dynamic light scattering is a non-destructive, high-throughput analysis of the aggregation state of a purified drug substance [35]. This equipment was used by BCM [32] and MIT [10] for size and structural control; hence, it was included in the investment costs. UV-Vis-Spectrophotometer, specific *P. pastoris* ELISA's kits to test binding, electrophoresis gels, western blots, and blotting reader were also included in the quality control equipment.

One disadvantage of the *K. phaffii* or *P. pastoris* expression host is that it requires methanol to induce the production of the recombinant protein. The methanol-inducible promoter PAOX1 is tightly regulated, and it is the most common way of producing recombinant proteins. However, handling methanol should be done carefully as it is a highly flammable liquid. Although the containers operate at a much lower scale than industrial large-scale facilities, it is still important to take quality guidelines into consideration. First, methanol can be safely stored in high density polyethylene (SUE) instead of stainless steel [54]. As usual, it should be kept in a well-ventilated area, away from ignition sites. Moreover, the methanol container should be capable of containing at least 110 % of the volume of the liquid and should be designed in accordance with NFPA 3 [36]. Alcohol resistant foam should be present in the container in case of a spill [36]. It is worth mentioning that several studies have also developed modified strains of *K. phaffii* to induce the protein production with other carbon sources such as sorbitol and estrogen [6, 10], which removed the need of methanol usage for protein induction.

2 Detailed Container Design

2.1 mRNA process

In order to ensure the feasibility of production with the spacial constraints given by the mobile units, we drafted exemplary layouts of the containers. The mRNA container layout is given in Figure 1 of the main text. This layout has previously been described in detail in [15]. Due to the small fluid volumes processed, the reactor and downstream processing equipment require only little space. The space required for downstream equipment can be further reduced to a wall segment of 1.75 m width by using a common fluid handling system for all unit operations and manually mounting new single use items for each processing step as described in Section 4.1 of [15]. The sizing of larger pieces of equipment such as the LNP formation device and the automated filling station was obtained from manufacturers. Storage space was estimated for four categories: Ambient storage of SUE and solids, cold storage of raw materials and the affinity resin [47] at 8 °C, frozen storage of raw materials at -20 °C and product storage at -80 °C. The resin required for 100 batches is assumed to be stored in 100 prepacked columns, each of which is 5 cm long according to [25] and a volume of 680 cm^3 according to our simulation. Assuming each column to be packaged in a 15 cm × 15 cm × 15 cm package, they can be stored in a 650 L refrigerator along with the raw materials stored at that temperature. Most raw materials require storage at -20 °C. Their combined (fluid) volume amounts to 15 L for 100 batches. We conservatively reserve a 650 L freezer these materials in the container design. Further, we include a high-performance freezer of outer dimensions of 198.1 cm height, 100.6 cm width and 95.5 cm depth for intermediate product storage, enabling to store up to to 21 batches or 210,000 doses at a time at -80 °C. We assume product storage in 10-dose-vials that are packed in 25-vial packages of 50 mm height and 125 mm width and depth. Similarly as for the resin, we calculate the storage space of SUE by assuming package dimensions and additionally dividing by an assumed storage efficiency of 50 - 90 %. We also include storage space for empty vials. These indeed require the most space of all items.

According to our SuperPro Designer simulation, we require about 50 L of RNase-free water for the process itself. We assume to additionally require the same amount of water for cleaning purposes. When using two sequentially connected RiOs 16 systems, one in its standard reverse osmosis configuration, and one one equipped with a 5,000 Da ultrafiltration cartridge, as suggested in [46], a production of up to 320 L $day^{-}1$ can be achieved.

The HVAC unit was chosen based on its ability to move more than the 20-fold container volume of air within one hour and its ability to maintain a sufficiently cold temperature inside of the container. The unit should be mounted on the container roof after shipping and may stay operational during road transport. The heat transport through the container wall can be estimated based on a constant heat transport coefficient for shipping containers of 0.4 W $m^{-2}K^{-}1$ [18, 57], and an average temperature difference across the container wall of 15 K. The additional heat generated inside the container by equipment and staff can be estimated based on the equipment's electricity demand and a rule of sum, respectively. Overall, a tonnage of 0.46 tons is required for the more demanding of the two containers. We conservatively choose to use a 2-ton HVAC system for each container.

We found the electricity consumption to be dominated by that of the refrigerators, freezers and the HVAC system with only a small fraction coming from actual process equipment. This is not surprising, considering the small fluid volumes and mild temperatures used. Overall, a single layer of battery packs under each container floor provides 189 kWh of storage capacity per container and enables 5.7 days to 7.6 days of grid-independent operation if the containers are connected, depending on whether or not production is taking place [15]. The combined peak power of the batteries of 128 kW for the two containers is sufficient to power the containers that have exhibit a combined peak power of 31 kW, if all equipment was to draw its peak demand at the same time.

2.2 Yeast process

Analogue to the mRNA process, a MOD unit for the yeast process was designed as shown in Figure 3. The space constraint is mainly determined by the amount of liquid medium and methanol that can be stored in the production container. Around 216 liters of sterilized medium and 123 liters of methanol can be stored in single use bags. These quantities are sufficient to supply the train of bioreactors with medium or methanol during 18 batches, which is equivalent to 75 days. The liquid medium should be stored at room temperature in the dark. The shelf life of this solution is approximately one year. Hence, its storage should not represent an issue for this process. The medium is prepared in the mixer in Single Use bags and it is sterilized by filtration.

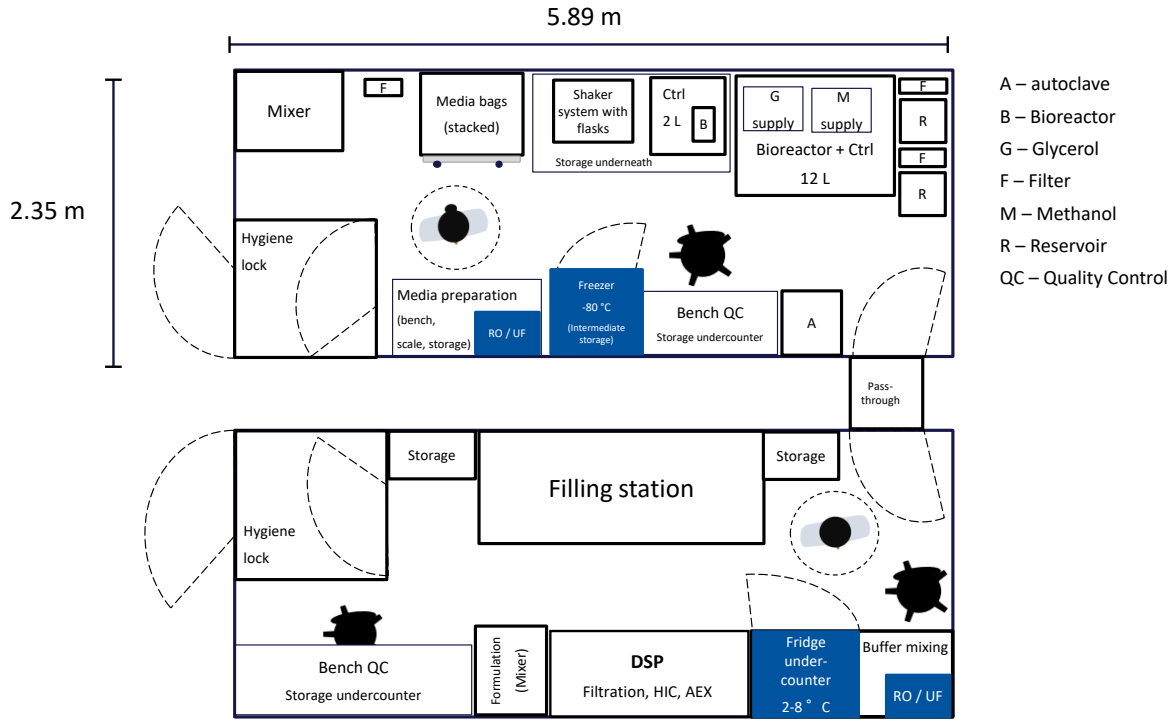

Fig. 3: Schematic layout of the yeast containers. Container dimensions shown are the inner dimensions.

3 Sensitivity Analysis

Many factors affecting the final cost per dose are challenging to predict accurately. Some technical assumptions need to be verified using a pilot plant and the cost of many raw materials cannot be known before negotiations respecting the precise terms of the agreement. Therefore, we conduct a sensitivity analysis, that is, we assess the final cost per dose for cases where individual factors are at the limits of their realistic range. The result of such an analysis can be found in Figure 2 of the main text. Additionally, the interaction of different impact factors can be visualised in a two-dimensional plant using a countour plots.

In Fig. 4, the sensitivity of production scale and effective dose size on the final vaccine costs is visualised. The batch size is considered infeasible as it surpasses 1 g mRNA, and 0.9 protein per batch, respectively for the two processes. Therefore, the feasible process scale depends on the dose size of the specific vaccine produced. Possible doses of mRNA range from 30 μg for the BioNTech/Pfizer vaccine to 100 μg for the Moderna vaccine. For yeast-based COVID-19 vaccines, dose sizes from 15 to 50 μg

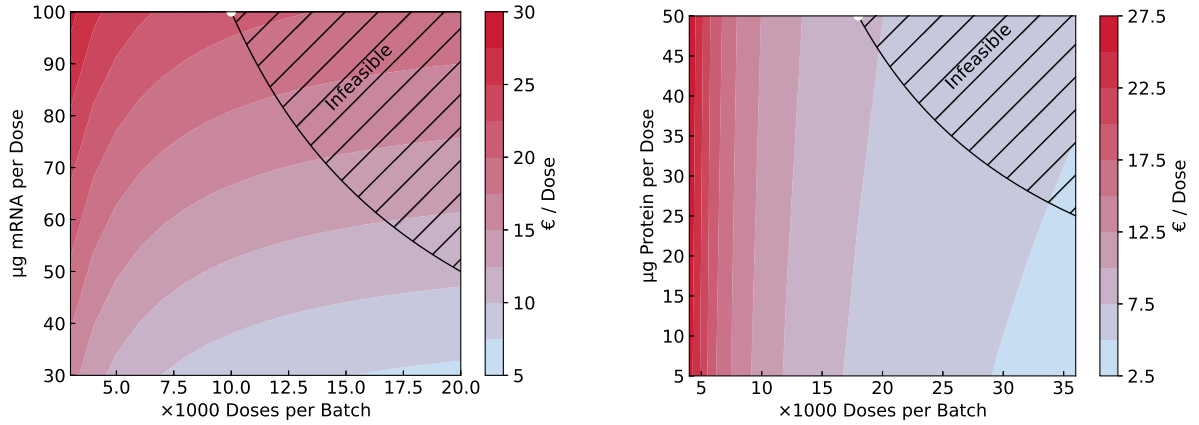

(a) mRNA (b) Yeast

Fig. 4: Sensitivity of dose size and batch scale on cost per dose of mRNA (a) and yeast-based (b) vaccine. The white point marks the chosen operation point for this work; The black markings indicate feasibility limits of MOD concept, which depends on the dose size required. It is assumed that 100 batches are produced

protein per dose are currently investigated in clinical trials [20]. Manual handling of the buffer volume limits further scale-up of the mRNA process and if this is overcome, even further scale-up will require a larger TFF system. Note, however, that the limitation is based on the chosen technology and may be overcome through innovation or through omitting the space limitation given by two containers. For the yeast process, the limitation of the batch size arises from limiting the reactor size to a maximum of 50 L, again, based on the spacial limitations given by the container environment. In a scenario in which the amount of protein or mRNA per dose tends towards the lower end, the limitation may shift from the reaction and or purification to the filling and packaging step, as this scales with the number of doses, rather than with the amount of product produced. For large-scale processes, the filling step has been identified as the scale-limiting step, before [31].

The chart shows that for batch sizes below approximately 10,000 doses or mRNA and 20,000 doses of yeast-based vaccine, there is a strong incentive to produce larger batches, whereas above that, this incentive decreases. As expected, developing a vaccine requiring low dose size is advantageous it allows to produce a larger number of doses per batch. Additionally, for the mRNA vaccine, the dose size has a significant effect on cost per dose at a fixed number of doses per batch. This effect is much less pronounced for yeast, where those cost factors that dependent of the dose size, such as raw materials and resins, only account for a small share of the total costs.

4 Additional Facility Location Example - Namibia

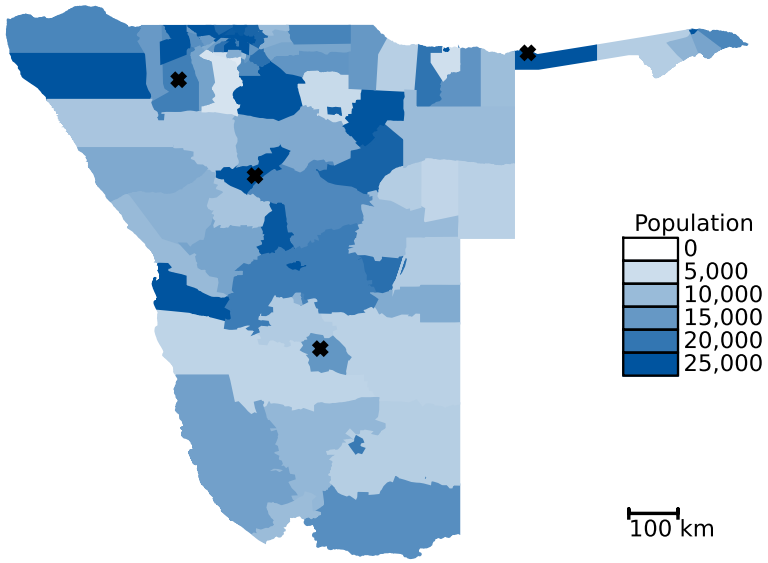

Fig. 5: Optimisation-based distribution of mRNA production containers in Namibia.

Figure 5 shows the optimal container distribution using the minimum number of containers (see Section 2.4 of the main text) for Namibia. Due to its low population density, the country requires only four production units consisting of two containers each. Moving these containers in between batches becomes much more interesting for this case as compared to Nigeria but it outside the scope of our analysis.

5 Data Tables

In the following tables, we present some of the major cost data used in our analysis. The costs are divided in investment cost, cost for consumable materials as defined in the main text and raw materials. Unlisted equipment cost and wiring cost are included as 30 % and 10 % of equipment costs, respectively. Building costs are accounted for by adding 250 % of equipment purchase costs, not including turnkey equipment, e.g., refrigerators. Rows printed in bold font are categories summarizing the rows below.

Table 1: Investment costs mRNA process

Categorie	**Units**	**Cost per unit**	**Investment cost**
Container	**2**	**3,083 €**	**6,167 €**
Interior construction container	**-**	**-**	**186,748 €**
Hygiene lock (doors, walls)	2	13,074 €	**26,148 €**
Wall panelling	**28**	**80 €**	**2,240 €**
Floor scaffolding	1	25,000 €	**25,000 €**
Lighting (LED panels)	8	396 €	**3,167 €**
AC/DC converter	**2**	**5,000 €**	**10,000 €**
Pass through	1	4,380 €	**4,380 €**
Table	3	1,271 €	**3,813 €**
Battery	14	8,000 €	**112,000 €**
Tangential flow filtration	**1**	**38,740 €**	**38,740 €**
Chromatography	**-**	**-**	**450 €**
Flow-trough heater	1	450 €	**450 €**
Dolomite Telos LNP device	**1**	**44,190 €**	**44,190 €**
Meros high speed microscope	1	13,290 €	13,290 €
Telos support frame	1	4,250 €	4,250 €
Flow sensor	2	1,600 €	3,200 €
Mitos quad pump	1	14,400 €	14,400 €
Software	1	1,520 €	1,520 €
Telos remote chamber	3	2,510 €	7,530 €
Sterile filtration	**-**	**-**	**4,203 €**
Pump	1	4,203 €	4,203 €
Quality control	**-**	**-**	**89,886 €**
Gel electrophoresis	1	800 €	800 €
Bio-Dot	1	1,300 €	1,300 €
Vacuum pump	1	1,437 €	1,437 €
Blotting reader	1	22,349 €	22,349 €
Dynamic light scattering	1	55,000 €	55,000 €
UV-vis-spectrophotometer	1	8,000 €	8,000 €
Computers (QC and others)	1	1,000 €	1,000 €
Filling system	**1**	**750,000 €**	**750,000 €**
Cooling systems	**-**	**-**	**40,699 €**
Raw material freezer	1	7,384 €	7,384 €
Product freezer (-80°C)	1	19,323 €	19,323 €
Refrigerator (intermed / POROS® resin)	2	6,996 €	13,992 €
HVAC system with HEPA filter	**2**	**9,996 €**	**19,992 €**
Filter system with fan	1	1,100 €	1,100 €
RNAse-free water production	**-**	**-**	**13,320 €**
Reverse osmosis system (also for UF)	2	6,660 €	13,320 €
Shipping costs of containers	**-**	**-**	**12,000 €**
ship transport	2	5,000 €	10,000 €
road transport / km	2000	1 €	2,000 €
Setting up the container on site	**1**	**10,000 €**	**10,000 €**
Building costs	**1**	**532,265 €**	**532,265 €**
Unlisted process equipment purchase cost	**1**	**303,391 €**	**303,391 €**
Unlisted auxiliary equipment purchase cost	**1**	**57,874 €**	**57,874 €**
Wiring costs	**1**	**156,548 €**	**156,548 €**

Table 2: Consumables costs mRNA process

Tasks	**Units per batch**	**Cost per unit**	**OPEX per batch**
Reactor	**1**	**446 €**	**446 €**
Tangential flow filtration	**-**	**-**	**1,985 €**
Cartridge	3	662 €	1,985 €
Chromatography	**-**	**-**	**31,508 €**
Column	1	1,778 €	1,778 €
POROS® resin	0.68	43,720 €	29,730 €
Dolomite Telos	**-**	**-**	**59,470 €**
Telos clamp module	10	4,930 €	49,300 €
Linear connector tunnel	1	300 €	300 €
Telos fittings pack	1	440 €	440 €
Telos plug set	1	420 €	420 €
Telos chip FFKM seal	10	96 €	960 €
Telos FFKM O-Ring	1	150 €	150 €
Telos 2 reagent encapsulation chip SC	10	790 €	7,900 €
Sterile filtration	**-**	**-**	**900 €**
Cartridge	1	900 €	900 €
Disposable clean room suits	5	**130 €**	**650 €**
Vials	**1000**	**2 €**	**1,730 €**
RNAse-Free water production	**-**	**-**	**90 €**
Progard pretreatment pack	0	457 €	0 €
Ultrafiltration cartridge (Pyrogard D)	1	90 €	90 €
Bags	**1**	**1,266 €**	**1,266 €**
Other	**1**	**1,000 €**	**1,000 €**
Labor / h	**32**	**80 €**	**2,560 €**

Table 3: Raw material costs mRNA process

	Material costs	**Amount per batch / g**	**OPEX per batch**
0.1 M ATP[a]	149.47 € g^{-1}	14.56	2,175.80 €
0.1 M CleanCap	2,500.00 € g^{-1}	11.83	29,566.96 €
0.1 M CTP[b]	149.67 € g^{-1}	14.56	2,178.71 €
0.1 M GTP[c]	150.24 € g^{-1}	14.56	2,187.08 €
0.1 M UTP[d]	149.91 € g^{-1}	14.56	2,182.23 €
1 mg $mL^{-}1$ DNA template	745.63 € g^{-1}	7.28	5,427.15 €
DC-Cholesterol	960.00 € g^{-1}	4.65	4,461.45 €
DMG PEG-2000[e]	158.21 € g^{-1}	0.85	133.79 €
DOTAP[f]	1,300.00 € g^{-1}	7.85	10,201.53 €
DSPC[g]	150.00 € g^{-1}	1.78	266.29 €
EDTA[h]	0.26 € g^{-1}	3.34	0.86 €
Ethanol	0.09 € g^{-1}	446.98	40.97 €
Magnesiumdiacetate	0.27 € g^{-1}	1.13	0.30 €
Natriumacetatate	0.03 € g^{-1}	205.72	6.86 €
OmniPur® DTT	2.87 € g^{-1}	0.44	1.26 €
Pyrophosphatase	135.48 € g^{-1}	5.82	788.90 €
RNase Inhibitor	191.27 € g^{-1}	7.28	1,392.14 €
Sodium Chloride	0.08 € g^{-1}	153.84	12.05 €
Spermidine	30.60 € g^{-1}	0.09	2.69 €
T7 RNA Polymerase	557.88 € g^{-1}	46.58	25,987.27 €
Tris HCl	0.41 € g^{-1}	19.86	8.11 €
Triton-X-100	0.13 € g^{-1}	0.59	0.07 €

[a] Adenosine-5'-Triphosphate [b] Cytidine-5'-Triphosphate [c] Guanosine-5'-Triphosphate [d] Uridine-5'-Triphosphate
[e] 1,2-dimyristoyl-rac-glycero-3-methoxypolyethylene glycol-2000 [f] 1,2-dioleoyl-3-trimethylammonium-propane
[g] 1,2-distearoyl-sn-glycero-3-phosphocholine [h] ethylenediaminetetraacetic acid

Table 4: Investment costs yeast process

Categorie	Units	Cost per unit	Investment costs
Container	**2**	**3,083 €**	**6,167 €**
Interior construction container	**-**	**-**	**186,748 €**
Hygiene lock (doors, walls)	2	13,074 €	26,148 €
Wall panelling	**28**	**80 €**	**2,240 €**
Floor scaffolding with floor	1	25,000 €	25,000 €
Lighting (LED panels)	8	396 €	3,167 €
AC/DC converter	**2**	**5,000 €**	**10,000 €**
Pass through	1	4,380 €	4,380 €
Table	3	1,271 €	3,813 €
Battery	14	8,000 €	112,000 €
Shaker system	**-**	**-**	**10,093 €**
500mL erlenmeyer flask clamp	1	75 €	75 €
1L erlenmeyer flask clamp	1	106 €	106 €
Mixer (buffer and formulation)	2	4,956 €	9,912 €
Tangential flow filtration system	**1**	**38,740 €**	**38,740 €**
Chromatography	**-**	**-**	**65,447 €**
Chromatography system	1	65,447 €	65,447 €
Sterile filtration	**1**	**4,203 €**	**4,203 €**
Pump	1	4,203 €	4,203 €
Quality control	**1**	**90,510 €**	**90,510 €**
Gel electrophoresis	1	800 €	800 €
Vacuum pump	1	1,437 €	1,437 €
Blotting reader	1	22,349 €	22,349 €
Dynamic light scattering	1	55,000 €	55,000 €
UV-vis-spectrophotometer	1	8,000 €	8,000 €
Computers (QC and others)	1	1,000 €	1,000 €
ELISA kit	1	670 €	670 €
Air compressor	2	627 €	1,254 €
Filling system	**1**	**750,000 €**	**750,000 €**
Cooling systems	**-**	**-**	**12,736 €**
Interm. freezer (-80°C)	1	9,688 €	9,688 €
Fridge (2 -8 °C)	1	3,048 €	3,048 €
HVAC system with HEPA filter	**2**	**9,996 €**	**19,992 €**
Filter system with fan	1	1,100 €	1,100 €
RNAse-free water production	**2**	**13,320 €**	**26,640 €**
Reverse osmosis system (also for UF)	2	6,660 €	13,320 €
Shipping costs	**1**	**12,000 €**	**12,000 €**
Setting up the container on site	**1**	**10,000 €**	**10,000 €**
Building costs	**1**	**532,265 €**	**532,265 €**
Unlisted process equipment purchase cost	**1**	**299,511 €**	**299,511 €**
Unlisted auxiliary equipment purchase cost	**1**	**57,874 €**	**57,874 €**
Wiring costs	**1**	**121,127 €**	**121,127 €**

Table 5: Consumables costs yeast process

Tasks	**Units per batch**	**Cost per unit**	**OPEX per batch**
Shake flasks (plastic and disposable)	**4**	**46 €**	**92 €**
Shake flask 500 mL	2	18 €	36 €
Shake flask 1 L	2	28 €	56 €
Reactor	**2**	**37,584 €**	**37,584 €**
SUT 5 L	1	12,000 €	12,000 €
SUT 12 L	1	-	-
Oxygen sensor	2	-	-
pH sensor	2	-	-
Tangential flow filtration	**-**	**-**	**1,925 €**
Cartridge 0.1 um, 30 cm	1	795 €	795 €
Cartridge 5 kDa, 41 cm	2	565 €	1,130 €
Chromatography SUT	**-**	**-**	**19,027 €**
HIC SUT (L)	1.48	10,882 €	16,105 €
AEC SUT (L)	0.31	9,426 €	2,922 €
Sterile filtration	**-**	**-**	**2,626 €**
Cartridge 0.2 um	2	900 €	1,800 €
Cartridge 0.2 um (long, for sterilisation of 50 L)	1	826 €	826 €
Disposable cleanroom suits	**28**	**130 €**	**3,640 €**
Vials	**1800**	**2 €**	**3,114 €**
RNAse-free water production	**-**	**-**	**547 €**
Progard pretreatment pack	0	457 €	0 €
Ultrafiltration cartridge (Pyrogard D)	1	90 €	90 €
Buffer bottles SUT and storage	**-**	**-**	**1,118 €**
HIC buffers (2)	2	140 €	280 €
AEC buffer (1)	1	140 €	140 €
Single use bags for mixers	4	175 €	698 €
Standard bioprocessing bags	**1**	**1,720 €**	**1,720 €**
Other	**1**	**1,000 €**	**1,000 €**
Labor (h)	**195.42**	**80 €**	**15,634 €**

Table 6: Raw material costs yeast process

Bulk material	Material costs	Amount per batch / g	OPEX per batch
P. pastoris X33 strain	1 € g^{-1}	447	447 €
Potassium sulfate (g)	63 € g^{-1}	0.071	4 €
Magnesium sulfate heptahydrate (g)	51 € g^{-1}	0.129	7 €
Potassium hydroxide (g)	14 € g^{-1}	0.1644	2 €
Calcium sulfate dehydrate (g)	3 € g^{-1}	0.634	2 €
Glycerol (g)	500 € g^{-1}	0.168253968	84 €
Phosphoric acid (85 %) (ml/L)	131 € g^{-1}	1.012	132 €
Methanol (L) (kg = 5.2 kg)	7 € g^{-1}	57	374 €
YNB Media (PTM salts) (g)	23 € g^{-1}	3.54	83 €
Sodium Chloride (g)	70 € g^{-1}	0.17	12 €
Tris-HCl (g)	40 € g^{-1}	1.46	58 €
Ammonium Sulfate (g)	2,650 € g^{-1}	0.158	419 €
Alum (g)	14 € g^{-1}	0.992	13 €
CpG 1018 (g)	2660 € g^{-1}	9	23,940

References

[1] Annex 2: Who good manufacturing practices for biological products, 2016. URL https://www.who.int/biologicals/areas/vaccines/Annex_2_WHO_Good_manufacturing_practices_for_biological_products.pdf?ua=1.

[2] Stephane Bancel, Joseph William, John, Aunins, John Grant, and Tirtha Charkraborty. Manufacturing methods for production of rna transcripts.

[3] Francesco Berlanda Scorza, Yingx-ia Wen, Andrew Geall, and Frederick Porter. Rna purification methods, 2014.

[4] Anna K. Blakney, Paul F. McKay, Bárbara Ibarzo Yus, Yoann Aldon, and Robin J. Shattock. Inside out: optimization of lipid nanoparticle formulations for exterior complexation and in vivo delivery of sarna. *Gene Therapy*, 26(9):363–372, 2019.

[5] Vincent Brunner, Manuel Siegl, Dominik Geier, and Thomas Becker. Biomass soft sensor for a pichia pastoris fed-batch process based on phase detection and hybrid modeling. *Biotechnology and Bioengineering*, 117(9):2749–2759, 2020.

[6] Jicong Cao, Pablo Perez-Pinera, Ky Lowenhaupt, Ming-Ru Wu, Oliver Purcell, Cesar de La Fuente-Nunez, and Timothy K. Lu. Versatile and on-demand biologics co-production in yeast. *Nature communications*, 9(1):77, 2018.

[7] Wen-Hsiang Chen, Shivali M. Chag, Mohan V. Poongavanam, Amadeo B. Biter, Ebe A. Ewere, Wanderson Rezende, Christopher A. Seid, Elissa M. Hudspeth, Jeroen Pollet, C. Patrick McAtee, Ulrich Strych, Maria Elena Bottazzi, and Peter J. Hotez. Optimization of the production process and characterization of the yeast-expressed sars-cov recombinant receptor-binding domain (rbd219-n1), a sars vaccine candidate. *Journal of pharmaceutical sciences*, 106(8):1961–1970, 2017.

[8] Wen-Hsiang Chen, Xinrong Tao, Anurodh Shankar Agrawal, Abdullah Algaissi, Bi-Hung Peng, Jeroen Pollet, Ulrich Strych, Maria Elena Bottazzi, Peter J. Hotez, Sara Lustigman, Lanying Du, Shibo Jiang, and Chien-Te K. Tseng. Yeast-expressed sars-cov recombinant receptor-binding domain (rbd219-n1) formulated with aluminum hydroxide induces protective immunity and reduces immune enhancement. *Vaccine*, 38(47):7533–7541, 2020.

[9] cytiva. Combine chromatography techniques to optimize your protein purification, 2020. Accessed: 2021/10/01.

[10] Neil C. Dalvie, Andrew M. Biedermann, Sergio A. Rodriguez-Aponte, Christopher A. Naranjo, Harish D. Rao, Meghraj P. Rajurkar, Rakesh R. Lothe, Umesh S. Shaligram, Ryan S. Johnston, Laura E. Crowell, Seraphin Castelino, Mary Kate Tracey, Charles A. Whittaker, and J. Christopher Love. Scalable, methanol-free manufacturing of the sars-cov-2 receptor binding domain in engineered <em>komagataella phaffii</em&gt. *bioRxiv : the preprint server for biology*, page 2021.04.15.440035, 2021.

[11] R. Gordon Douglas, Vijay B. Samant, Stanley A. Plotkin, Walter A. Orenstein, Paul A. Offit, and Kathryn M. Edwards. The vaccine industry. *Plotkin's Vaccines*, pages 41–50.e1, 2018.

[12] Laura E. Easton, Yoko Shibata, and Peter J. Lukavsky. Rapid, nondenaturing rna purification using weak anion-exchange fast performance liquid chromatography. *RNA (New York, N.Y.)*, 16(3): 647–653, 2010.

[13] Pavlos C. Englezou, Cedric Sapet, Thomas Démoulins, Panagiota Milona, Thomas Ebensen, Kai Schulze, Carlos-Alberto Guzman, Florent Poulhes, Olivier Zelphati, Nicolas Ruggli, and Kenneth C. McCullough. Self-amplifying replicon rna delivery to dendritic cells by cationic lipids. *Molecular therapy. Nucleic acids*, 12:118–134, 2018.

[14] Amy S. Espeseth, Pedro J. Cejas, Michael P. Citron, Dai Wang, Daniel J. DiStefano, Cheryl Callahan, Gregory O' Donnell, Jennifer D. Galli, Ryan Swoyer, Sinoeun Touch, Zhiyun Wen, Joseph Antonello, Lan Zhang, Jessica A. Flynn, Kara S. Cox, Daniel C. Freed, Kalpit A. Vora, Kapil Bahl, Andrew H. Latham, Jeffrey S. Smith, Marian E. Gindy, Giuseppe Ciaramella, Daria Hazuda, Christine A. Shaw, and Andrew J. Bett. Modified mrna/lipid nanoparticle-based vaccines expressing respiratory syncytial virus f protein variants are immunogenic and protective in rodent models of rsv infection. *NPJ vaccines*, 5:16, 2020.

[15] Steffen Fahr, Lukas Thiel, and Carl Sengoba. Mobile on-demand (mod) mrna vaccine mobile on-demand (mod) mrna vaccine production: A design and optimal location study, 2021. URL https://web.fe.up.pt/~fgm/eurecha/scp_2020/eurecha2020_mainreport_1stprize.pdf.

[16] Owen S. Fenton, Kevin J. Kauffman, Rebecca L. McClellan, James C. Kaczmarek, Manhao D. Zeng, Jason L. Andresen, Luke H. Rhym, Michael W. Heartlein, Frank DeRosa, and Daniel G. Anderson. Customizable lipid nanoparticle materials for the delivery of sirnas and mrnas. *Angewandte Chemie International Edition*, 57(41):13582–13586, 2018.

[17] Rafael G. Ferreira, Neal F. Gordon, Rick Stock, and Demetri Petrides. Adenoviral vector covid-19 vaccines: Process and cost analysis. *Processes*, 9(8), 2021.

[18] Ludmiła Filina-Dawidowicz and Sergiy Filin. Innovative energy-saving technology in refrigerated containers transportation. *Energy Efficiency*, 12(5):1151–1165, 2019.

[19] Leonidas Gkionis, Richard A. Campbell, Harmesh Aojula, Lynda K. Harris, and Annalisa Tirella. Manufacturing drug co-loaded liposomal formulations targeting breast cancer: Influence of preparative method on liposomes characteristics and in vitro toxicity. *International journal of pharmaceutics*, 590:119926, 2020.

[20] Government of India. Permission to conduct clinical trial of new drug or investigational new drug, 2020.

[21] Maria L. Guevara, Francesca Persano, and Stefano Persano. Advances in lipid nanoparticles for mrna-based cancer immunotherapy. *Frontiers in chemistry*, 8:589959, 2020.

[22] Kimberly J. Hassett, Kerry E. Benenato, Eric Jacquinet, Aisha Lee, Angela Woods, Olga Yuzhakov, Sunny Himansu, Jessica Deterling, Benjamin M. Geilich, Tatiana Ketova, Cosmin Mihai, Andy Lynn,

Iain McFadyen, Melissa J. Moore, Joseph J. Senn, Matthew G. Stanton, Örn Almarsson, Giuseppe Ciaramella, and Luis A. Brito. Optimization of lipid nanoparticles for intramuscular administration of mrna vaccines. *Molecular therapy. Nucleic acids*, 15:1–11, 2019.

[23] Jordana M. Henderson, Andrew Ujita, Elizabeth Hill, Sally Yousif-Rosales, Cory Smith, Nicholas Ko, Taylor McReynolds, Charles R. Cabral, Julienne R. Escamilla-Powers, and Michael E. Houston. Cap 1 messenger rna synthesis with co-transcriptional cleancap® analog by in vitro transcription. *Current protocols*, 1(2):e39, 2021.

[24] Invitrogen Corporation. Pichia fermentation process guidelines, 2002. URL https://tools.thermofisher.com/content/sfs/manuals/pichiaferm_prot.pdf. Accessed: 09/11/2021.

[25] ISSA, William, Joseph, AUNINS, John, Grant, and Stephane Bancel. Ribonucleic acid purification, 2014.

[26] Mehmedalija Jahic, Andres Veide, Theppanya Charoenrat, Tuula Teeri, and Sven-Olof Enfors. Process technology for production and recovery of heterologous proteins with pichia pastoris. *Biotechnology Progress*, 22(6):1465–1473, 2006.

[27] Katalin Karikó, Hiromi Muramatsu, János Ludwig, and Drew Weissman. Generating the optimal mrna for therapy: Hplc purification eliminates immune activation and improves translation of nucleoside-modified, protein-encoding mrna. *Nucleic acids research*, 39(21):e142, 2011.

[28] Robin Kastilan, Alexander Boes, Holger Spiegel, Nadja Voepel, Ivana Chudobová, Stephan Hellwig, Johannes Felix Buyel, Andreas Reimann, and Rainer Fischer. Improvement of a fermentation process for the production of two pfama1-dico-based malaria vaccine candidates in pichia pastoris. *Scientific Reports*, 7(1):11991, 2017.

[29] Zoltán Kis, Robin Shattock, Nilay Shah, and Cleo Kontoravdi. Emerging technologies for low-cost, rapid vaccine manufacture. *Biotechnology journal*, 14(1):e1800376, 2019.

[30] Zoltán Kis, Cleo Kontoravdi, Antu K. Dey, Robin Shattock, and Nilay Shah. Rapid development and deployment of high-volume vaccines for pandemic response. *Journal of advanced manufacturing and processing*, 2(3):e10060, 2020.

[31] Zoltán Kis, Cleo Kontoravdi, Robin Shattock, and Nilay Shah. Resources, production scales and time required for producing rna vaccines for the global pandemic demand. *Vaccines*, 9(1), 2020.

[32] Jungsoon Lee, Zhuyun Liu, Wen-Hsiang Chen, Junfei Wei, Rakhi Kundu, Rakesh Adhikari, Joanne Altieri Rivera, Portia M. Gillespie, Ulrich Strych, Bin Zhan, Peter J. Hotez, and Maria Elena Bottazzi. Process development and scale-up optimization of the sars-cov-2 receptor binding domain–based vaccine candidate, rbd219-n1c1. *Applied Microbiology and Biotechnology*, 105(10):4153–4165, 2021.

[33] Gilda Lemos-Pérez, Sheila Chávez-Valdés, Hany González-Formental, Giselle Freyre-Corrales, Amalia Vázquez-Arteaga, Beatriz Álvarez-Acevedo, Lismary Ávila-Díaz, Ricardo U. Martínez-Rosales, Yahima Chacón-Quintero, Edelgis Coizeau-Rodríguez, Ariel Palenzuela-Díaz, Enrique Noa-Romero, and Gerardo E. Guillén-Nieto. Elevated antibody titers in abdala vaccinees evaluated by elecsys® anti-sars-cov-2 s highly correlate with umelisa sars-cov-2 anti rbd, ace-2 binding inhibition and viral neutralization assays. *medRxiv*, 2021.

[34] Wallace Woon-Fong Leung. *Centrifugal separations in biotechnology*. Butterworth-Heinemann, 2020.

[35] J. Christopher Love, Kerry Routenberg Love, and Paul W. Barone. Enabling global access to high-quality biopharmaceuticals. *Current Opinion in Chemical Engineering*, 2(4):383–390, 2013. Biotechnology and bioprocess engineering / Process systems engineering.

[36] Enrique Medina and Robert R. Roberts. Methanol safe handling manual - 4th edition, 2017. URL https://www.methanol.org/wp-content/uploads/2017/03/Safe-Handling-Manual.pdf.

[37] Jennifer Nelson, Elizabeth W. Sorensen, Shrutika Mintri, Amy E. Rabideau, Wei Zheng, Gilles Besin, Nikhil Khatwani, Stephen V. Su, Edward J. Miracco, William J. Issa, Stephen Hoge, Matthew G. Stanton, and John L. Joyal. Impact of mrna chemistry and manufacturing process on innate immune activation. *Science advances*, 6(26):eaaz6893–eaaz6893, 2020.

[38] Jeroen Pollet, Wen-Hsiang Chen, and Ulrich Strych. Recombinant protein vaccines, a proven approach against coronavirus pandemics. *Advanced drug delivery reviews*, 170:71–82, 2021.

[39] Cristina Poveda, Amadeo B. Biter, Maria Elena Bottazzi, and Ulrich Strych. Establishing preferred product characterization for the evaluation of rna vaccine antigens. *Vaccines*, 7(4), 2019.

[40] Precision NanoSystems. NanoAssemblr GMP system, 2020. URL https://www.precisionnanosystems.com/platform-technologies/product-comparison/gmp-system. Accessed: 2021/03/16.

[41] M. B. Pykhtina, V. P. Romanov, S. M. Miroshnichenko, and A. B. Beklemishev. Construction of a pichia pastoris strain efficiently producing recombinant human granulocyte-colony stimulating factor (rhg-csf) and study of its biological activity on bone marrow cells. *Molecular Biology Reports*, 47(1): 607–620, 2020.

[42] Anand Ramanathan, G. Brett Robb, and Siu-Hong Chan. mrna capping: biological functions and applications. *Nucleic acids research*, 44(16):7511–7526, 2016.

[43] Robert E. Rhoads. *Synthetic mRNA*, volume 1428. Springer New York, New York, NY, 2016.

[44] Justin M. Richner, Sunny Himansu, Kimberly A. Dowd, Scott L. Butler, Vanessa Salazar, Julie M. Fox, Justin G. Julander, William W. Tang, Sujan Shresta, Theodore C. Pierson, Giuseppe Ciaramella, and Michael S. Diamond. Modified mrna vaccines protect against zika virus infection. *Cell*, 168(6):1114–1125.e10, 2017.

[45] Axel Schmidt, Heribert Helgers, Florian Lukas Vetter, Alex Juckers, and Jochen Strube. Digital twin of mrna-based sars-covid-19 vaccine manufacturing towards autonomous operation for improvements in speed, scale, robustness, flexibility and real-time release testing. *Processes*, 9(5), 2021.

[46] Ichiro Kano Stéphane Mabic. Production of ultrapure water for rnase-sensitive applications via ultrafiltration, 2012.

[47] Thermo Scientific. POROS™ Oligo (dT)25 Affinity Resin, 2020. URL https://www.thermofisher.com/order/catalog/product/A47382?de&en#/A47382?de&en. Accessed: 2021/03/03.

[48] V. Looser, B. Bruhlmann, F. Bumbak, C. Stenger, M. Costa, A. Camattari, D. Fotiadis, and K. Kovar. Cultivation strategies to enhance productivity of pichia pastoris: A review. *Biotechnology Advances*, 33(6, Part 2):1177–1193, 2015.

[49] Sriram Vaidyanathan, Krist T. Azizian, A. K. M. Ashiqul Haque, Jordana M. Henderson, Ayal Hendel, Sabrina Shore, Justin S. Antony, Richard I. Hogrefe, Michael S. D. Kormann, Matthew H. Porteus, and Anton P. McCaffrey. Uridine depletion and chemical modification increase cas9 mrna activity and reduce immunogenicity without hplc purification. *Molecular therapy. Nucleic acids*, 12: 530–542, 2018.

[50] Amelie Vallet-Courbin, Mélusine Larivière, Agnès Hocquellet, Audrey Hemadou, Sarjapura-Nagaraja Parimala, Jeanny Laroche-Traineau, Xavier Santarelli, Gisèle Clofent-Sanchez, Marie-Josée Jacobin-Valat, and Abdelmajid Noubhani. A recombinant human anti-platelet scfv antibody produced in pichia pastoris for atheroma targeting. *PLOS ONE*, 12(1):e0170305, 2017.

[51] Jieliang Wang, Ying Peng, Haiyue Xu, Zhengrong Cui, and Robert O. Williams. The covid-19 vaccine race: Challenges and opportunities in vaccine formulation. *AAPS PharmSciTech*, 21(6):225, 2020.

[52] Watson Marlow. Fpc60: Fill/finish-system mit einzigartigen konfigurationsmöglichkeiten, 2021. URL https://www.wmftg.com/de-de/range/flexicon/fully-automatic-filling/fpc60-vial-filling-system/. Accessed: 2021/03/26.

[53] Drew Weissman, Norbert Pardi, Hiro Muramatsu, and Katalin Karikó. Hplc purification of in vitro transcribed long rna. *Methods in molecular biology (Clifton, N.J.)*, 969:43–54, 2013.

[54] World Health Organization. Health and safety guide no. 105: Methanol health and safety guides, 1997.

[55] Lior Zangi, Kathy O. Lui, Alexander von Gise, Qing Ma, Wataru Ebina, Leon M. Ptaszek, Daniela Später, Huansheng Xu, Mohammadsharif Tabebordbar, Rostic Gorbatov, Brena Sena, Matthias Nahrendorf, David M. Briscoe, Ronald A. Li, Amy J. Wagers, Derrick J. Rossi, William T. Pu, and Kenneth R. Chien. Modified mrna directs the fate of heart progenitor cells and induces vascular regeneration after myocardial infarction. *Nature biotechnology*, 31(10):898–907, 2013.

[56] Zifu Zhong, Séan Mc Cafferty, Francis Combes, Hanne Huysmans, Joyca de Temmerman, Arlieke Gitsels, Daisy Vanrompay, João Portela Catani, and Niek N. Sanders. mrna therapeutics deliver a hopeful message. *Nano Today*, 23:16–39, 2018.

[57] Ewelina Złoczowska. Maritime containers refrigeration plant faults survey. *New Trends in Production Engineering*, 1(1):589–595, 2018.